s-wave-scattering resonances induced by dipolar interactions of polar molecules

Zhe-Yu Shi, Ran Qi, and Hui Zhai[*]

Institute for Advanced Study, Tsinghua University, Beijing, 100084, China

We show that the *s*-wave-scattering resonances induced by dipolar interactions in polar molecular gases have a universal large and positive effective range, which is very different from Feshbach resonances previously realized in cold atoms before, where the effective range is either negligible or negative. Such a difference has important consequences in many-body physics. At a high-temperature regime, a positive effective range gives rise to a stronger repulsive interaction energy for positive scattering length, and a weaker attractive interaction energy for negative scattering length. At low temperatures, we study a polaron problem formed by a single-impurity molecule, and we find that the polaron binding energy increases at the BEC side and decreases at the BCS side. All these effects are opposite to narrow Feshbach resonances, where the effective range is negative.

A polar molecular gas with a strong dipolar interaction is a system of great interest to both the atomic and molecular physics and condensed-matter physics communities. The recent development of the stimulated Raman adiabatic passage (STIRAP) technique has succeeded in creating a nearly degenerate gas of KRb molecules in its rovibrational ground state [1]. Unfortunately, the KRb molecules are not stable against two-body decay into K_2 and Rb_2 molecules [2]. Recently, a theoretical calculation predicted that this problem can be avoided by choosing other combinations of alkali-metal atoms, such as KCs, KNa, NaCs, NaRb, and RbCs [3]. Applying the STIRP technique to these species is now occurring in many different laboratories all over the world. It is very promising that degenerate polar molecular gases can be realized within the next few years.

For these molecules their electric dipole moments can be polarized by an external electric field (say, along the $\hat{z}$ direction). As the applied electric field increases, the dipole moment d continuously increases from zero to the permanent dipole moment, and different molecules have different values of permanent dipole moment [4]. Therefore the two-body interaction potential studied here can be modeled as

$$V_D(\mathbf{r}) = \begin{cases} \frac{d^2(1-3\cos^2\theta)}{r^3}, & r > r_c, \\ \infty, & r < r_c, \end{cases} \quad (1)$$

which contains a long-range dipolar interaction and a short-range nonuniversal potential. θ is the angle between $\hat{r}$ and $\hat{z}$. Here, for simplicity, we use a hard-core potential to mimic the short-range behavior of a very complicated realistic potential, where r_c is the core size. We can introduce a length scale $D = md^2/(2\hbar^2)$, and then the typical dipole energy is given by $\hbar^2 D/(2m\langle r\rangle^3) \approx (k_F D)E_F$. By controlling the electric field, one can tune $k_F D$ from zero to the regime $k_F D \approx 1$ [4], i.e., the dipole energy is comparable to the Fermi energy.

Understanding the two-body problem of two strongly interacting quantum dipoles is an important step toward understanding the rich many-body physics of this system. Previously, the dipolar interaction effects in the high partial-wave channel have been studied extensively, for instance, the

p-wave pairing [5,6] and *p*-wave and *d*-wave Fermi-surface distortion [5,7]. The dipolar interaction effects in the *s*-wave channel have not been well studied, because they always vanish in simple mean-field treatments.

In fact, previous studies have shown that, as D increases, each partial-wave channel will display a series of resonances where the scattering length of each partial-wave channel diverges, and we call them dipolar interaction-induced resonances (DIIRs) [8–10]. Among all these channels, resonances in the *s*-wave channel are the most pronounced. However, both the two-body properties and the many-body physics at DIIRs have not been completely understood. In this Rapid Communication we study both the two-body properties of DIIRs and two many-body problems of two-component fermionic molecules across a DIIR, which is a high-temperature regime with equal population, and a single impurity in a fully polarized Fermi gas. From these studies we want to emphasize the significant difference between an *s*-wave DIIR and other *s*-wave resonances. The main conclusions are summarized as follows:

(i) Near the *s*-wave resonances the effective range r_0 is large and positive. This is qualitatively different from a magnetically tuned Feshbach resonance (MFR) studied before, where r_0 is either negligible (wide MFR) or large but negative (narrow MFR). Across different DIIRs, r_0/D is a universal function of D/a_s and $r_0/D \approx 1.84$ at resonance. Therefore $k_F r_0$ is of the order of unity and the effect of r_0 cannot be ignored in many-body physics.

(iii) At high temperature, the attractive interaction energy of a DIIR is significantly smaller for negative scattering length a_s compared to a wide MFR, while for positive a_s, in the upper branch, the repulsive energy of DIIR is much larger. Both can be understood by analyzing the energy dependence of the scattering length or the two-body energy levels.

(iii) At low temperature, we consider a polaron formed by a single-impurity molecule immersed in the Fermi sea. We find that the polaron binding energy is larger compared to a wide MFR at the BEC side and the resonance regime, while it is smaller at the BCS side.

Two-body problem. Using D as the length unit $r \rightarrow r/D$ and $E_D = \hbar^2/(mD^2)$ as the energy unit $E \rightarrow E/E_D$, the two-body Schrödinger equation can be written in dimensionless

————
[*]hzhai@mail.tsinghua.edu.cn

form as

$$\left[-\frac{1}{2}\nabla^2 + \frac{1 - 3\cos^2\theta}{r^3} \right] \Psi = E\Psi \qquad (2)$$

in the regime $r > r_c$ and the boundary condition is given by $\Psi(r = r_c) = 0$. Expanding the wave function in terms of spherical harmonics as $\Psi(r,\theta,\varphi) = \sum_{lm}\frac{1}{r}R_{lm}(r)Y_{lm}(\theta,\varphi)$, the Schrödinger equation can be reduced to

$$-\frac{1}{2}\frac{d^2}{dr^2}R_{lm} + \frac{1}{r^2}H^m_{l,l'}(r)R_{l'm}(r) = ER_{lm}, \qquad (3)$$

where $H^{(m)}_{ll'} = l(l+1)\delta_{ll'} + \langle Y_{lm}|(1 - 3\cos^2\theta)|Y_{l'm}\rangle/r$. $H_{ll'}$ couples all l to $l \pm 2$ and m is still a good quantum number. Moreover, since the dipolar coupling decays $(1/r^3)$ faster than the centrifugal barrier term $(1/r^2)$, at large distance, coupling between different l effectively vanishes. The asymptotic behavior of the scattering wave function still can be decoupled as different partial-wave channels, so one can introduce a scattering length for each partial-wave channel [11,12].

Here we will focus on the s-wave channel since it has no centrifugal barrier and the interaction effect is expected to be the strongest. However, it is easy to note that $H_{00} = 0$, which means one cannot obtain any interaction effect if directly projecting the Schrödinger equation (2) into the $|l,m\rangle = |0,0\rangle$ state. The interaction effect in the s-wave channel comes from its coupling to a higher partial-wave channel. Following a simple second-order perturbation argument, one can obtain an effective potential from a virtual process between $|0,0\rangle$ and $|2,0\rangle$,

$$-\frac{\langle 00|(1 - 3\cos^3\theta)|20\rangle\langle 20|(1 - 3\cos^2\theta)|00\rangle\frac{D^2}{r^6}}{\frac{6}{r^2}} \propto -\frac{D^2}{r^4}.$$

Hence, as D increases, the effective potential becomes deeper and deeper, which introduces a series of bound states and causes scattering resonances. This is the basic mechanism of DIIR. Since the energies of those intermediate states for this induced interaction are $\hbar^2 l(l+1)/(m\langle r\rangle^2) \gg 2E_F$ for $l = 2,4,6,\ldots$, we expect that the presence of a Fermi sea and the Pauli blocking effect will not strongly affect the induced interaction, which justifies using the induced interaction in many-body studies.

Following Ref. [10], we first diagonalize the matrix $H_{ll'}$ by a unitary matrix $X(r)$ as $X^\dagger(r)H(r)X(r) = \Lambda(r)$. Translating the radial wave function as $\Phi_l = X^\dagger_{ll'}R_{l'}$, Eq. (3) will become

$$-\frac{1}{2}\frac{d^2}{dr^2}\Phi_l + q_{ll'}(r)\frac{d}{dr}\Phi_{l'} + v_{ll'}(r)\Phi_{l'} = E\Phi_l, \qquad (4)$$

where $q(r) = -\frac{1}{2}X^\dagger(r)dX(r)/dr$ and $v(r) = \Lambda(r)/r^2 - \frac{1}{2}X^\dagger(r)d^2X(r)/dr^2$. At a large distance, because $H(r)$ becomes effectively diagonal, X becomes an identity matrix and Φ_l still has the same asymptotic behavior as R_l. At an intermediate and short distance, the diagonal part of $v(r)$ contains the centrifugal potential contribution for all $l \neq 0$, which separates the s-wave from other partial waves. Because of this energy separation, we can take the approximation that only keeps the diagonal terms of $q_{ll'}$ and $v_{ll'}$. The infinite number of the coupled differential equation of Eq. (3) is reduced to a set of decoupled equations

$$-\frac{1}{2}\frac{d^2}{dr^2}\Phi_l + q_{ll}(r)\frac{d}{dr}\Phi_l + v_{ll}(r)\Psi_l = E\Phi_l. \qquad (5)$$

In Eq. (5), $v_{00}(r) \neq 0$ is the induced interaction in the s-wave channel. Numerically solving Eq. (5) for $l = 0$, we obtain
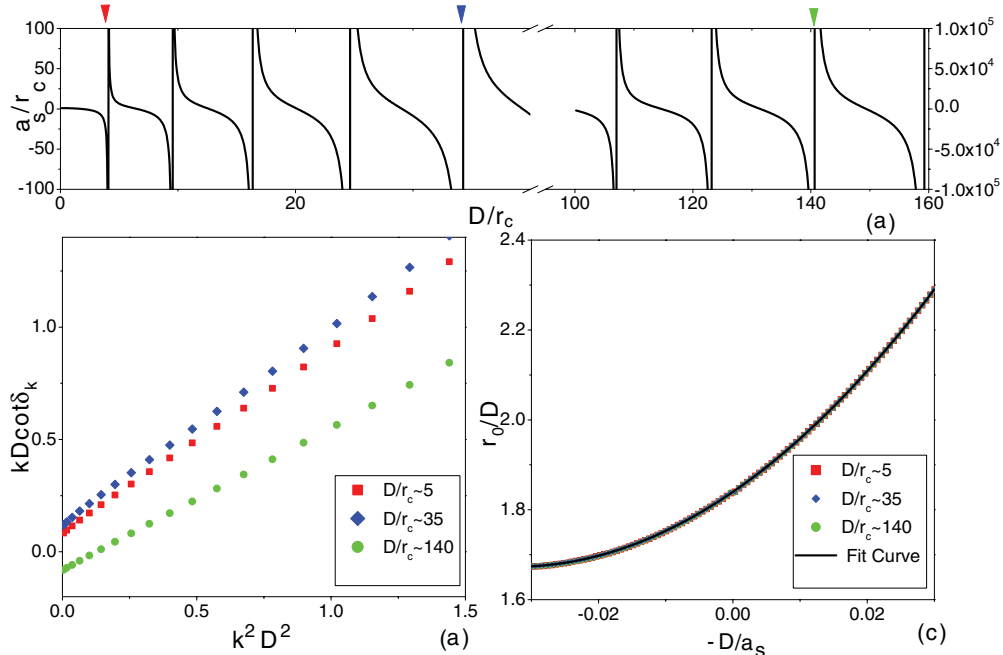

FIG. 1. (Color online) (a) Scattering length a_s/r_c as a function of D/r_c. (b) $kD\cot\delta_k$ as a function of $(kD)^2$ at different D/r_c as marked in (a). (c) r_0/D as a function of $-D/a_s$ across different resonances.
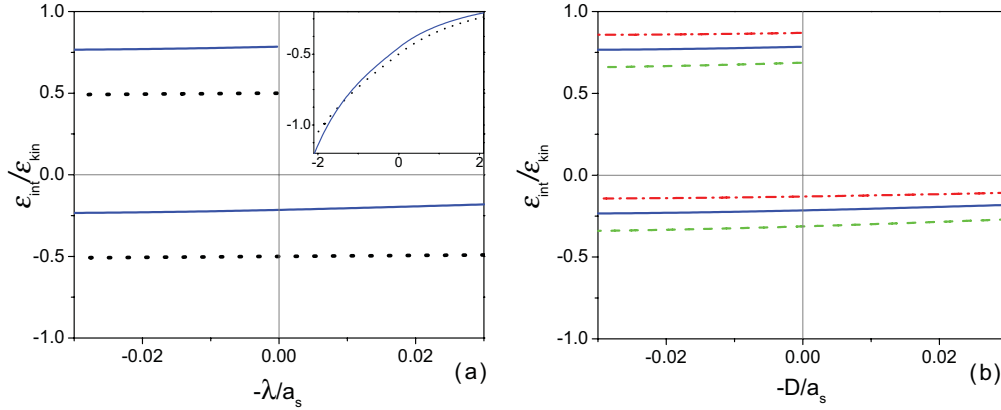
FIG. 2. (Color online) (a) $\epsilon_{\text{int}}/\epsilon_{\text{kin}}$ as a function of $-\lambda/a_s$ for a DIIR (solid line) and a wide MFR (dotted line). $\lambda/D = 1$. Inset: The same plot for $\lambda/D = 70$. (b) $\epsilon_{\text{int}}/\epsilon_{\text{kin}}$ for DIIR with different temperatures. $\lambda/D = 2$ (green dashed line), $\lambda/D = 1$ (blue solid line), and $\lambda/D = 0.5$ (red dotted-dashed line). Positive $\epsilon_{\text{int}}/\epsilon_{\text{kin}}$ at the positive a_s side excludes the contribution from the bound state.

its asymptotic behavior of $\Phi_{l=0}$ as $\sin(kr + \delta_k)$, where $k = \sqrt{2mE}/\hbar$.

Scattering resonances and effective range. Once we obtain an *s*-wave phase shift from solving Eq. (5), we can define the *s*-wave scattering length as $a_s = -\lim_{k\to 0} \tan\delta_k / k$. We plot a_s/r_c as a function of D/r_c in Fig. 1(a). It displays a series of resonances as D/r_c increases, and the resonance window in the D/r_c axes gets wider for larger D/r_c. The locations of the resonances can be determined by an intuitive WKB estimation [10]. This approach precisely captures all *s*-wave resonances with relatively wide windows [9], and misses some extremely narrow ones which are due to a bound state in an even higher partial-wave channel and are coupled to an *s*-wave channel by the ignored off-diagonal coupling in $q_{ll'}$ and $v_{ll'}$. We ignore them because they are too narrow to be studied experimentally.

We expand the phase shift as $k \cot\delta_k = -1/a_s + r_0 k^2/2 + \cdots$. In Fig. 1(b) we find that $kD\cot\delta_k$ is a very good linear function of $(kD)^2$, and the positive slope means that r_0 is *positive*. In Fig. 1(c), we plot r_0/D as a function of D/a_s for different resonances with different D/r_c. It is very remarkable that all these curves across different resonances perfectly coincide with each other, which shows that r_0/D is a universal function of D/a_s. In other words, the short-range physics (r_c/D) is irrelevant in determining r_0. Inspired by the relation between the effective range and the physical range of a square-well potential, we fit the curve by $r_0/D = \alpha_0 + \alpha_1 D/a_s + \alpha_2 (D/a_s)^2$, and find $\alpha_0 = 1.8390 \pm 0.0006$, $\alpha_1 = -10.168 \pm 0.002$, and $\alpha_2 = 158.2 \pm 0.1$. All the high-order coefficients are several orders of magnitudes smaller. At resonance, $r_0 \approx 1.84D$. Noting that D can be of the same order of $1/k_F$, we can therefore realize resonances in a cold atom system with a large and positive effective range. This is very important for using cold atoms to simulate nuclei and neutron matter [13].

High-temperature regime. In the remainder of this Rapid Communication, we will investigate the many-body effects of a positive effective range. We shall compare DIIR with a zero-range model for a wide MFR, which gives a constant

phase shift of $k \cot\delta_k = -1/a_s$ for all k, and $r_0 = 0$. First, we study the high-temperature regime by a second-order virial expansion, because the resonant interaction manifests itself in the interaction energy even above a degenerate temperature, and can be measured easily by the spectroscopy method.

By second-order virial expansion, we have

$$b_2 = \sum e^{|E_b|/(k_b T)} + \int_0^{+\infty} \frac{dk}{\pi} \frac{d\delta_k}{dk} e^{-\lambda^2 k^2/(2\pi)}, \qquad (6)$$

where we have ignored all the contributions from high partial waves, and $\lambda = \sqrt{2\pi\hbar^2/(mk_b T)}$. The interaction energy is given by

$$\epsilon_{\text{int}} = \frac{3k_b T n}{2}(n\lambda^3)\left[-\frac{b_2}{\sqrt{2}} + \frac{\sqrt{2}}{3}T\frac{\partial b_2}{\partial T} \right]. \qquad (7)$$

In Fig. 2(a), we compare $\epsilon_{\text{int}}/\epsilon_{\text{kin}}$ for a DIIR with a wide MFR, and in Fig. 2(b) we show $\epsilon_{\text{int}}/\epsilon_{\text{kin}}$ for a DIIR with different temperatures, where $\epsilon_{\text{kin}} = 3k_b T n(n\lambda^3)/2$. On the side with $a_s > 0$, negative ϵ_{int} includes the contribution from the bound state, while positive ϵ_{int} excludes the bound-state contribution, which corresponds to the physics of "the upper branch."

First, for scattering states, it is known that $\epsilon_{\text{int}}/\epsilon_{\text{kin}}$ approaches ∓ 0.5 as one approaches a wide MFR from the negative and positive side of a_s [14]. For a DIIR, we find for $a_s < 0$ that the attractive interaction energy is weaker for a DIIR, and for $a_s > 0$, the repulsive interaction energy is stronger. This is strongly in contrast to a narrow MFR $(r_0 < 0)$ where the opposite effect is found by Ref. [15]. This can be understood from an argument based on the energy dependence on scattering length. Let us consider a situation where a_s not very close to resonance, and r_0 is nonzero, but is still small compared to λ^2/a_s. Because $a(\bar{k}) = 1/(1/a_s - r_0\bar{k}^2/2)$ ($\bar{k}$ denotes a thermal average of k, and is of the order of $1/\lambda$), for $a_s < 0$, one finds $|a(\bar{k})| < |a_s|$ for $r_0 > 0$, and $|a(\bar{k})| > |a_s|$ for $r_0 < 0$; for $a_s > 0$, one finds $|a(\bar{k})| > |a_s|$ for $r_0 > 0$, and $|a(\bar{k})| < |a_s|$ for $r_0 < 0$. This is consistent
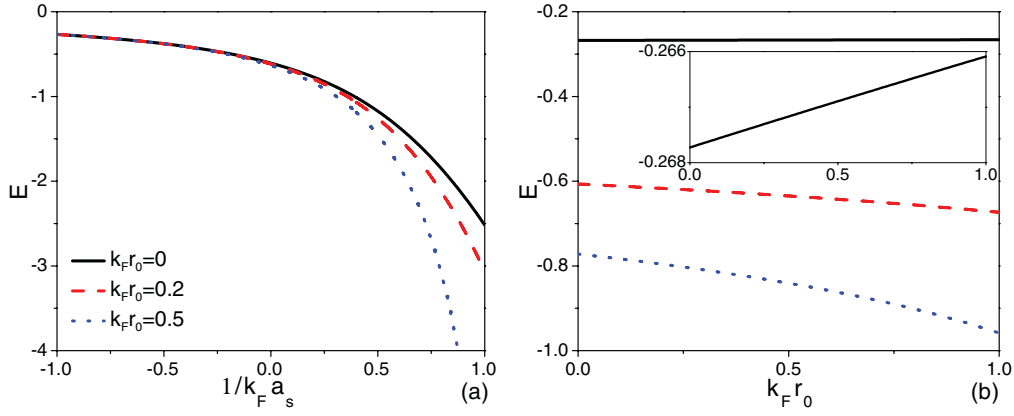
FIG. 3. (Color online) (a) Polaron energy $\mathcal{E}/E_F$ as a function of $-1/(k_F a_s)$ for $k_F r_0 = 0$ (wide resonance, solid line), $k_F r_0 = 0.2$ (dashed line), and $k_F r_0 = 0.5$ (dotted line). (b) $\mathcal{E}/E_F$ as a function of $k_F r_0$ for $1/(k_F a_s) = -1$ (solid line), $1/(k_F a_s) = 0$ (dashed line), and $1/(k_F a_s) = 0.2$ (dotted line).

with r_0 dependence of the interaction energy shown in Fig. 2(a).

An alternative way to understand this result is through analyzing energy levels. Let us consider two molecules confined in a large hard sphere so that the two-body wave function $\psi(r)$ has to vanish at $r = R$. The energy levels of the s-wave states are determined by $E_n = \hbar^2 k_n^2/m$, where k_n satisfies the equation $k_n R + \delta_{k_n} = n\pi$. In the limit $a_s \to 0^-$, $\delta_k = 0$ and $k_n^{0^-} = n\pi/R$, while for $a_s \to 0^+$, $\delta_k = \pi$ and $k_n^{0^+} = (n-1)\pi/R$. For a wide MFR, at resonance, $\delta_k = \pi/2$, and all k_n is given by $(n-1/2)\pi/R$, which is responsible for $\epsilon_{int}/\epsilon_{kin} = \pm 0.5$ at resonance [15]. For a DIIR, at resonance, k satisfies $kR + \arctan[2/(r_0 k)] = n\pi$. At a given temperature, the system is dominated by states with $k \sim 1/\lambda$. Hence, $\arctan[2/(r_0 k)]$ is always smaller than $\pi/2$ if $r_0 > 0$ and it decreases to zero as the temperature increases. Therefore, the downshifts of the energy levels $E_n^{0^-} - E_n$ are smaller compared to a wide MFR, and they decrease as the temperature increases. The upshifts of the energy levels $E_n - E_n^{0^+}$ are larger compared to a wide MFR, and they increase as the temperature increases. This is also consistent with the temperature dependence of $\epsilon_{int}/\epsilon_{kin}$ as shown in Fig. 2(b).

The effective range r_0 also has an effect on the bound-state energy. The bound-state energy is given by the pole of scattering amplitude $f(E) = 1/(1/a_s - r_0 E/2 - i\sqrt{E})$, which gives

$$E = -\frac{\hbar^2}{m a_s^2} \frac{1 - \sqrt{1 - 2r_0/a_s}}{r_0/a_s} \simeq -\frac{\hbar^2}{m a_s^2}\left(1 + \frac{r_0}{2a_s}\right). \quad (8)$$

For the same a_s, the binding energy $|E|$ is larger with positive r_0. For the same reason, for a narrow MFR with negative r_0, the binding energy is smaller. In the inset of Fig. 2(a) we show that at a lower temperature, the attractive interaction energy of a DIIR will finally exceed that of a wide MFR. This is because, for a lower temperature, the contribution of the lowest bound state will gradually become dominant, and the larger binding energy finally overwhelms the smaller contribution from the scattering states.

Single-impurity problem at low temperature. In general, the low-temperature many-body physics at resonance is too sophisticated to be studied by a simple method. Here, in order to illustrate that the effect of r_0 at low temperature could be different from that in high temperatures, we consider a simpler situation where one single-impurity molecule is dressed by a Fermi sea of majority molecules and forms a polaron. For wide resonance, such a problem can be well described by a variational wave function or T-matrix approach [16]. Here we apply a similar approach to DIIR and obtain the following self-consistent equation for polaron energy $\mathcal{E}$:

$$\mathcal{E} = \sum_{|\mathbf{q}|<|\mathbf{k}_F|} \frac{1}{\frac{Vm}{4\pi}\left[\frac{1}{a_s} - \frac{mr_0}{2}\left(\mathcal{E} + \epsilon_{\mathbf{q}}^{\uparrow} - \epsilon_{\mathbf{q}}^{b}\right)\right] + I(\mathcal{E})}, \quad (9)$$

where $I(\mathcal{E},\mathbf{q}) = \sum_{|\mathbf{k}|>k_F}\left(\frac{1}{\epsilon_{\mathbf{k}}^{\uparrow} + \epsilon_{\mathbf{p}+\mathbf{q}-\mathbf{k}}^{\downarrow} - \epsilon_{\mathbf{q}}^{\uparrow} - \epsilon_{\mathbf{p}}^{\downarrow} - \mathcal{E}} - \frac{1}{\epsilon_{\mathbf{k}}^{r}}\right) - \sum_{|\mathbf{k}|<k_F}\frac{1}{\epsilon_{\mathbf{k}}^{r}}$, $\epsilon_{\mathbf{k}}^{r} = \mathbf{k}^2/m$, and $\epsilon_{\mathbf{k}}^{b} = \mathbf{k}^2/(4m)$. The details for obtaining this equation are similar as the same impurity problem across a narrow MFR [17]. We find that the effective range has a more dramatic effect on polaron binding energy at the BEC side than at the BCS side, as shown in Fig. 3(a). We find that at the BCS side, a positive r_0 will decrease the polaron binding energy $|\mathcal{E}|$ while it will increase $|\mathcal{E}|$ at the resonance regime and the BEC side. Such an effect is also opposite to the polaron near a narrow MFR [17], and for narrow resonances, such an effect has been observed in a recent experiment [18]. In both cases, it is caused by and can be understood from the energy dependence on the scattering length [17]. It will be very interesting to observe the countereffect in dipolar gases of polar molecules, so that the effects of the effective range in many-body systems will be established in a comprehensive way.

[1] K.-K. Ni, S. Ospelkaus, M. H. G. de Miranda, A. Pe'er, B. Neyenhuis, J. J. Zirbel, S. Kotochigova, P. S. Julienne, D. S. Jin, and J. Ye, Science **322**, 231 (2008); S. Ospelkaus, K.-K. Ni, G. Quemener, B. Neyenhuis, D. Wang, M. H. G. de Miranda, J. L. Bohn, J. Ye, D. S. Jin, Phys. Rev. Lett. **104**, 030402 (2010).

[2] S. Ospelkaus, K.-K. Ni, D. Wang, M. H. G. de Miranda, B. Neyenhuis, G. Quner, P. S. Julienne, J. L. Bohn, D. S. Jin, and J. Ye, Science **327**, 853 (2010); K.-K. Ni, S. Ospelkaus, D. Wang, G. Quemener, B. Neyenhuis, M. H. G. de Miranda, J. L. Bohn, J. Ye, and D. S. Jin, Nature (London) **464**, 1324 (2010).

[3] P. S. Źuchowski and J. M. Hutson, Phys. Rev. A **81**, 060703(R) (2010).

[4] Using the permanent dipole moment calculated by M. Aymar and O. Dulieu, J. Chem. Phys. **122**, 204302 (2005), we estimate that the largest D attainable is 9.3 μm for KCs, 7.3 μm for KNa, 49.4 μm for NaCs, 17.7 μm for NaRb, and 4.7 μm RbCs, hence, one can tune D from zero for those values far exceeding the interparticle distance by the electric field. For a typical density of polar molecules, the density is $n \approx 10^{11}$ cm^{-3} and therefore $k_{\mathrm{F}} \approx 2 \ \mu$m^{-1}.

[5] For a review, see M. A. Baranov, Phys. Rep. **464**, 71 (2008).

[6] For instance, see L. You and M. Marinescu, Phys. Rev. A **60**, 2324 (1999); M. A. Baranov, M. S. Marénko, V. S. Rychkov, and G. V. Shlyapnikov, *ibid*. **66**, 013606 (2002); C. Wu and J. E. Hirsch, Phys. Rev. B **81**, 020508 (2010); N. R. Cooper and G. V. Shlyapnikov, Phys. Rev. Lett. **103**, 155302 (2009).

[7] For instance, see T. Miyakawa, T. Sogo, and H. Pu, Phys. Rev. A **77**, 061603(R) (2008); J. N. Zhang and S. Yi, *ibid*. **80**, 053614 (2009); B. M. Fregoso and E. Fradkin, Phys. Rev. Lett. **103**, 205301 (2009); C. K. Chan, C. Wu, W. C. Lee, and S. Das Sarma, Phys. Rev. A **81**, 023602 (2010).

[8] M. Marinescu and L. You, Phys. Rev. Lett. **81**, 4596 (1998); B. Deb and L. You, Phys. Rev. A **64**, 022717 (2001).

[9] K. Kanjilal and D. Blume, Phys. Rev. A **78**, 040703 (2008).

[10] V. Roudnev and M. Cavagnero, J. Phys. B **42**, 044017 (2009); Phys. Rev. A **79**, 014701 (2009).

[11] S. Yi and L. You, Phys. Rev. A **61**, 041604(R) (2000); A. Derevianko, *ibid*. **67**, 033607 (2003).

[12] C. Chin, R. Grimm, P. Julienne, and E. Tiesinga, Rev. Mod. Phys. **82**, 1225 (2010).

[13] An alternative proposal of generating resonance with a positive effective range can be found in B. Marcelis, B. Verhaar, and S. Kokkelmans, Phys. Rev. Lett. **100**, 153201 (2008).

[14] T. L. Ho and E. J. Mueller, Phys. Rev. Lett. **92**, 160404 (2004).

[15] T. L. Ho and X. L. Cui, e-print arXiv:1105.4627.

[16] F. Chevy, Phys. Rev. A **74**, 063628 (2006); R. Combescot, A. Recati, C. Lobo, and F. Chevy, Phys. Rev. Lett. **98**, 180402 (2007).

[17] R. Qi and H. Zhai, e-print arXiv:1112.1282.

[18] C. Kohstall, M. Zaccanti, M. Jag, A. Trenkwalder, P. Massignan, G. M. Bruun, F. Schreck, and R. Grimm, e-print arXiv:1112.0020.